Flow Rate Dependence of Soil Hydraulic Characteristics

D. Wildenschild,* J. W. Hopmans, J. Simunek

ABSTRACT

The rate dependence of unsaturated hydraulic characteristics was analyzed using both steady state and transient flow analysis. One-step and multistep outflow experiments, as well as quasi-static experiments were performed on identical, disturbed samples of a sandy and a loamy soil to evaluate the influence of flow rate on the calculated retention and unsaturated hydraulic conductivity curves. For the sandy soil, a significant influence of the flow rate on both the retention and unsaturated hydraulic conductivity characteristic was observed. At a given matric potential, more water was retained with greater applied pneumatic pressures. Matric potential differences of 10 to 15 cm (for given saturation) and water content differences of up to 7% (for given potential) could be observed between the slowest and the fastest outflow experiments, predominantly at the beginning of drainage. The hydraulic conductivity also increased with increasing flow rate for higher saturations, while a lower hydraulic conductivity was observed near residual saturation for the higher flow rates. We observed a continuously increasing total water potential gradient in the sandy soil as it drained, especially for high-pressure transient one-step experiments. This indicates a significant deviation from static equilibrium, as obtained under static or steady-state conditions. For the finer textured soil, these flow-rate dependent regimes were not apparent. A number of physical processes can explain the observed phenomena. Water entrapment and pore blockage play a significant role for the high flow rates, as well as lack of air continuity in the sample during the wettest stages of the experiment.

T HE TWO BASIC soil hydraulic characteristics controlling flow in unsaturated porous media are the retention characteristic, $\theta(h)$, and the unsaturated hydraulic conductivity characteristic, $K(h)$. Commonly, these characteristics are measured under static equilibrium or steady-state conditions and are subsequently applied to both steady-state and transient flow analyses, thereby assuming that the retention characteristic is not affected by nonequilibrium conditions. Thus, both equilibrium and steady-state measurements are routinely used to analyze transient flow phenomena and vice versa.

However, a number of experiments presented in the sixties and early seventies suggested that these assumptions might not be entirely justifiable. When comparing drying water retention data obtained by equilibrium, steady state, and transient methods, Topp et al. (1967) found that more water was retained in a sand at a given matric potential for the transient flow case than for the static equilibrium and steady-state cases. The authors referred to a study by Harris and Morrow (1964), who studied pendular rings in packs of relatively large uniform spheres, and found that some of the pores in the drained sphere pack remained full, as these became isolated from the bulk liquid before their air-entry pressure was attained. This bypassing of isolated liquid-filled pores explained the observed higher retained water content. An analogous explanation was suggested by Davidson et al. (1966) who investigated the dependence of the retention characteristic on the applied pressure increment during wetting. They reported a noticeable dependence of the equilibrium water content on the size of the applied pressure increment such that a higher water content was measured when small pressure increments were used during water absorption. The increase in water content was attributed to a reduction in the air volume entrapped during absorption if the soil was wetted at a slower rate. The authors concluded that the changes in water content should be treated as an immiscible displacement process, where the resistance to movement and spatial configuration of both water and air need not be single valued with respect to water content—a hypothesis stated previously by Nielsen et al. (1962).

Later, Smiles et al. (1971) carried out desorption experiments in a horizontal column of uniform soil and found that the relationship between the soil water matric potential and the water content was nonunique throughout the column. Vachaud et al. (1972) continued the work of Smiles et al. (1971) to determine if this same phenomenon occurred in vertical drainage of a uniform column of fine sand as well. They compared retention curves obtained under static and dynamic flow conditions and their results were consistent with those of Smiles et al. (1971). In particular, Vachaud et al. (1972) showed that a rate increase of matric potential with time reduced the volumetric outflow, thereby causing deviations from the static retention characteristic.

The issues of rate dependence of soil hydraulic properties have since been mostly disregarded. The unsaturated hydraulic conductivity dependence on flow conditions in particular has been the focus of few investigations, partly because of the tedious nature of its measurement; however, recent experiments carried out by Wildenschild et al. (1997), Plagge et al. (1999), Hollenbeck and Jensen (1999), and Schultze et al. (1999) support the notion that the flow regime may vary notably between different types of experiments, thereby influencing the estimation of the unsaturated hydraulic properties. In addition to the water retention characteristic, Plagge et al. (1999) investigated the influence of both flow rate and boundary condition type on the hydraulic conductivity function and concluded that experiments with larger water potential gradients tended to increase the unsaturated hydraulic conductivity. In experiments designed to in-

vestigate the influence of pore scale dead-end air fingers on relative permeabilities for air sparging in soils, Clayton (1999) found that the measured air permeabilities decreased with increasing displacement rate. Clayton attributed the displacement-rate dependent behavior to the development and subsequent breakthrough of dead-end air fingers. Most recently, Friedman (1999) concluded that the influence of flow velocity on the solid–liquid–gas contact angle could also explain the phenomena observed by Topp et al. (1967).

With the introduction of new and faster techniques for transient measurement of the hydraulic characteristics such as the one-step (Kool et al., 1985) and multi-step (van Dam et al., 1994; Eching et al., 1994) outflow methods, the question of the validity of these measurements has since become increasingly important. As many researchers now apply these faster techniques to determine the hydraulic characteristics of soils, it is important to examine the influence of the boundary conditions on the measurement results for these experiments. In many cases, recorded data of cumulative outflow as a function of time is combined with soil water matric potential head measured with a tensiometer at a point inside the sample (Eching et al., 1994) to facilitate inverse estimation of the hydraulic parameters. If the water content is dependent not only on the matric potential, but is also influenced by outflow rate, it needs to be taken into consideration when estimating the soil hydraulic properties. Outflow procedures are, however, not the only methods to be affected by this phenomenon. For the traditional static methods such as the pressure plate extraction method (Klute, 1986), soil water retention may be a function of the rate of flow between equilibrium points as well.

As improvements in measurement techniques, as well as the implementation of dynamic measurement methods, have become available, the aim of the present study was to continue the above referenced work. Using the currently available improved measurement techniques, we investigated the rate dependence of unsaturated hydraulic characteristics for two soils in short laboratory columns. Thus, the objective of this study was to investigate the influence of flow rate on soil hydraulic characteristics using both a direct and an inverse estimation method for two soils with different pore size distributions. The direct estimation is based on Darcy's Law (steady state), while the inverse estimation relies on numerical solution of Richards' equation and as such is a transient approach.

MATERIALS AND METHODS

Experimental Setup

A diagram of the flow cell and associated gas and water flow controls is shown in Fig. 1. The samples were packed in a pressure cell, 3.5-cm high and 7.62-cm diam. In addition to the top air inlet and the bottom water outlet, an extra outlet at the bottom was used to flush air bubbles from underneath the porous membrane. All connections consisted of quick disconnect fittings (Cole-Parmer, Delrin, 1/4-inch NPT, 06359-72) so that the cell could be detached for weighing. Weighing allowed for determination of the sample water content during
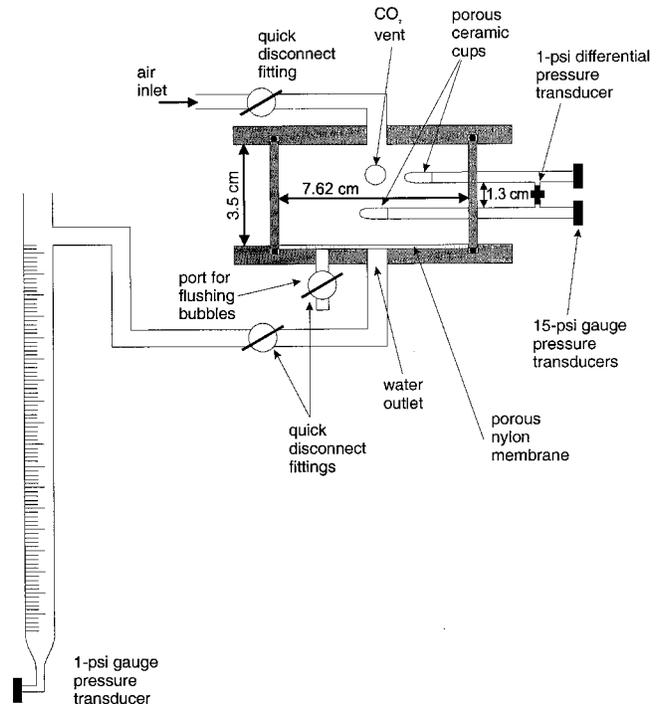
Fig. 1. Laboratory setup for outflow experiments.

the drainage experiment. Two tensiometers were inserted 1.1 and 2.4 cm from the bottom. The ports were offset laterally to minimize disturbance of flow between the tensiometers and to the overall flow in the sample. The tensiometers were made from 0.72-cm diam., 1-bar, high-flow tensiometer cups (Soil Moisture Corp. 652X03-BIM3), epoxyed to 1/4-inch diam. acrylic tubing. A short piece of smaller diameter brass tubing was used to support the connection of the tensiometer cup with the acrylic tubing. The tensiometers extend ≈2 cm into the sample. Two 15-psi transducers (136PC15G2, Honeywell, Minneapolis, MN) were used to monitor the matric potential head at the two locations. In addition, a 1-psi differential transducer (26PCAFA1D, Honeywell, Minneapolis, MN) was mounted to monitor the difference in matric potential between the two tensiometers, thus allowing computation of the hydraulic gradient. Two additional ports were added on opposite sides of the cell to vent the sample with CO_2 and allow full water saturation at the start of the outflow experiment.

The bottom outlet was connected to a burette for measuring the outflow as a function of time. The burette was mounted such that outflow water drained at atmospheric pressure. A 1-psi transducer (136PC01G2, Honeywell, Minneapolis, MN) was attached at the bottom of the burette to measure drained cumulative water volume. The upper boundary condition was controlled using regulated pressurized N. The N was bubbled through a distilled water reservoir before entering the pressure cell to minimize evaporation loss in the cell. Two layers of 1.2-micron, 0.1-mm thick nylon filters (Magna Nylon Membrane Filters, Micron Separations Inc., Westborough, MA) were used as a porous membrane at the bottom of the sample. We combined two nylon filters for a single porous membrane to reduce possible leaks thereby maintaining a bubble pressure of at least 700 cm during the outflow experiments. With a saturated hydraulic conductivity of ≈7.0 × 10^{-6} cm/s, the hydraulic resistance of the thin nylon membrane was low compared with other commonly used porous membranes, thereby minimizing water pressure differences across the porous membrane during drainage of the soil core. The experiments were

Table 1. Bulk physical properties of the investigated soils.

Soil type	Sand	Silt	Clay	Bulk density
		%		g/cm³
Columbia	63.2	27.5	9.3	1.45
Lincoln	88.6	9.4	2.0	1.69

conducted for two soils of varying textural composition, a Lincoln sand obtained from the EPAs RS Kerr Environmental Research Laboratory in Ada, OK, and a Columbia fine sandy loam collected along the Sacramento River near West Sacramento, CA. Soil properties for both soils are listed in Table 1 (Liu et al., 1998). The Columbia and Lincoln soil were sieved through 0.5- and 0.6-mm sieves, respectively, prior to packing. Each sample was packed only once for each series of experiments to minimize packing effects on the results. The soil was packed in the pressure cell in small increments and the cell tapped between each successive addition. Initial experiments with the Columbia soil showed some settling after a few wetting and drying cycles; therefore, the Columbia soil sample was vibrated for ≈1/2 hour after packing to obtain a well-settled sample.

Three different types of outflow experiments were performed. First, for the one-step experiments a single high pneumatic pressure was imposed on the soil sample to induce outflow. Second, multistep outflow experiments were carried out using identical procedures as for the one-step experiments except that a varying number of smaller pressure increments were applied instead of one large pressure step. Between each successively increasing pressure increment, time was allowed for the sample to equilibrate or for outflow to cease. In addition to the gas pressure induced outflow scenarios, a syringe pump procedure (Wildenschild et al., 1997) was used in a third series of experiments in which the soil sample was drained at a constant low flow rate, simulating quasi-static conditions at any time during the drainage experiment. A drainage rate of 0.5 ml/hr was used for the syringe pump measurements in both soils.

All experiments were started at an initial condition of $h_{bottom} \approx -2$ cm. Prior to each drainage experiment, the soil samples were resaturated using the same procedure every time (including the use of CO_2 to dissolve trapped air) to maintain identical initial saturation values between the different drainage experiments. Otherwise, observed differences could be attributed to varying initial conditions. The standard deviations of the initial sample weights representing variations of initial saturation were 0.962 g for six replicates of the Columbia soil and 0.732 g for 10 replicates of the Lincoln soil, representing water content variations of 0.0075 and 0.0050 cm³ cm⁻³ for the Lincoln soil and the Columbia soil, respectively.

Direct Estimation Using Darcy's Law

The retention characteristics for the soils were established from the average of the two tensiometer readings and the measured cumulative outflow volumes. The cumulative outflow was converted to sample average water content using soil porosity and assuming initial fully saturated conditions. At the conclusion of each experiment, the sample was weighed to determine final water content values, from which initial water content values were verified. This approach may introduce potential errors, since the measurements were carried out during transient conditions, thereby leading to possible depth variations in matric potential head, while a single core averaged water content was estimated from the cumulative outflow data. This could be of particular concern for the fast, one-step experiments where depth dependent matric potential

head gradients are most likely to occur. Also, the presence of the tensiometers in the sample could cause some disturbance of the flow field. As mentioned earlier, we believe that the small size and the offsetting of the tensiometers justify the assumption of one dimensionality.

The unsaturated hydraulic conductivity was estimated directly from Darcy's Law using various computational procedures. The tensiometer pair provided the hydraulic gradient in the center of the soil core as a function of drainage time, and when combined with the outflow rate provided the unsaturated hydraulic conductivity as a function of matric potential head or volumetric water content. To account for water flux density differences between the upper and lower parts of the soil sample during outflow, we used the method of Wendroth et al. (1993) to estimate the unsaturated hydraulic conductivity.

The soil sample was divided into three compartments as outlined in Fig. 2. The first (top) compartment (l_1) extended between the surface of the soil sample and the center between the two tensiometers, and was represented by the matric potential head measured in the first (top) tensiometer, h_1. The second compartment (l_2) extended from the center between the two tensiometers to the center between the lower tensiometer and the bottom of the soil sample. This second compartment was represented by the matric potential head measured with the second (lower) tensiometer, h_2. The third compartment (l_3) was defined by the bottom of the soil sample and the center between the lower tensiometer and the bottom of the sample. The matric potential head between the bottom of the sample and the lower tensiometer was assumed to be linearly distributed. Thus, this compartment was represented by the weighted mean of the matric potential head within the compartment $h_3 = h_{bottom} - (h_{bottom} - h_2)/4$. For each compartment, the water content at each time step was calculated from the representative matric potential head values (i.e., θ_1, θ_2, and θ_3).

For direct estimation of $K(\theta)$ or $K(h)$, the fluxes between the compartments were computed in two ways: either (1) from the top to the bottom, or (2) from the bottom to the top.

1. During the drainage experiments, the flux between compartments 1 and 2 (q_{12}) was computed from water storage changes between measurement times using θ_1, while the fluxes between compartments 2 and 3 (q_{23}) were computed from time rate of water storage changes using θ_1 and θ_2. Subsequently, $K_{12}(h)$ and $K_{23}(h)$ or $K_{12}(\theta)$ and $K_{23}(\theta)$ were estimated, assuming the Darcy equation to be valid, while substituting the representative matric po-
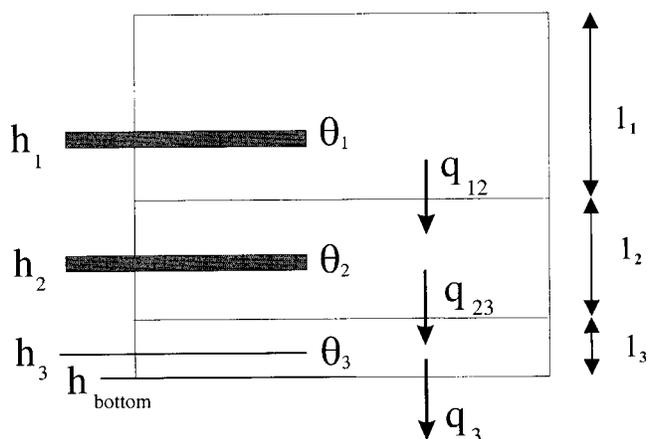
Fig. 2. Compartments and flux boundaries for the calculated hydraulic conductivities.

Table 2. Inversely estimated parameters for the Lincoln soil. (1.) estimated parameters: (α, n, K_s, θ_r), (2.) estimated parameters: (α, n, K_s, θ_r, l).

Date	SSQ	θ_r	α	n	K_s (cm/h)	l	R^2
			Onestep 0–250 mbar				
0611a	0.049	0.097	0.019	4.803	2.883		0.993
0611b	0.041	0.110	0.019	7.240	1.934	−0.282	0.996
			Onestep 0–125 mbar				
0531a	0.020	0.077	0.020	4.730	2.019		0.999
0531b	0.013	0.075	0.020	4.476	2.324	0.637	0.999
			Multistep 0–50–100 mbar				
0520a	0.051	0.041	0.023	3.104	0.911		0.998
0520b	0.029	0.095	0.022	5.882	0.363	−0.788	0.997
			Multistep 0–25–35–62–80–100 mbar				
0524a	0.014	0.050	0.021	3.749	0.588		0.999
0524b	0.010	0.072	0.021	4.420	0.413	−0.104	0.999
			Syringe pump (0.5 ml/h)				
0607b	0.008	0.043	0.022	3.402	1.349	−0.087	0.998

tential head values (h_1 and h_2 for q_{12}, and h_2 and h_3 for q_{23}). Finally, K_3 values were calculated directly from the bottom compartment drainage rate and matric potential gradients.

2. Alternatively, using the drainage rate from the bottom compartment, q_3, $K_3(h)$ was estimated from the Darcy equation, using h_2 and h_{bottom} to estimate the representative matric potential head gradient. Subsequently, $K_{32}(h)$ values and $K_{21}(h)$ values were calculated from fluxes between compartments 2 and 3 (q_{32}) and compartments 1 and 2 (q_{21}). These fluxes were estimated from q_3, after subtraction of the time rate of soil water storage changes of the representative compartments (obtained from time changes of θ_1, θ_2, and θ_3), and using the appropriate matric potential gradients.

To simplify the direct estimation results, we will only present data using a selection of experiments and conductivity estimations for each soil. For the Lincoln soil these experiments are one-step (0–250 mbar and 0–125 mbar), multistep (0–50–100 mbar and 0–25–35–62–80–100 mbar) and the quasi-static experiment. For the Columbia soil, we are presenting estimated data for one-step (0–500 mbar), multistep (0–250–500 mbar and 0–125–250–375–500 mbar), and the quasi-static experiment. In addition, we have chosen only to present data for the middle (K_{23} and K_{32}) and lower part (K_3) of the sample. This was done partly for simplicity, but also because the estimates from the upper part (K_{12} and K_{21}) were affected by the large gradients present towards the end of the experiments. For the multistep experiments in particular, this meant that the curves were discontinuous between individual pressure steps. Also, the estimates from the middle part of the sample (K_{23} and K_{32}) provide a more correct basis for comparison with the estimates based on the drainage rate (K_3), as opposed to the estimates from the upper part of the sample (K_{12} and K_{21}).

Unfortunately, it was not possible to estimate the hydraulic conductivity from the syringe pump experiments because the very small hydraulic gradients prevented accurate K estimation.

Inverse Estimation Based on Richards' Equation

The unsaturated hydraulic properties were inversely estimated using HYDRUS-1D (Simunek et al., 1998), which numerically solves Richards' equation in one dimension using a Galerkin-type linear finite element scheme. Minimization is accomplished using the Levenberg-Marquardt nonlinear

weighted least squares approach. The objective function was defined as the average weighted squared deviation normalized by the measurement variances of particular measurement sets. For additional details about inverse modeling, its application for estimation of soil hydraulic properties and the definition of the objective function, refer to Simunek et al. (1998), and Hopmans and Simunek (1999). For these experiments, the objective function contained matric potential head readings for the two tensiometers and cumulative outflow data measured as a function of time. The expressions of van Genuchten (1980) were used to parameterize the hydraulic functions

$$S_e = \frac{(\theta - \theta_r)}{\theta_s - \theta_r} = [1 + (\alpha|\psi|)^n]^{-m}$$

$$K = K_s S_e^l [1 - (1 - S_e^{1/m})^m]^2 \qquad [1]$$

where S_e is effective saturation, θ_s, θ_r and θ are full, residual and actual water contents, α, n and l are constants, $m = 1 - 1/n$, ψ is matric potential, and K and K_s are unsaturated and saturated hydraulic conductivities. The parameters optimized were either (α, n, K_s, θ_r) or (α, n, K_s, θ_r, l) where l is the exponent in Mualem's (1976) equation. The exponent is commonly fixed at a value of 0.5, however, the fit to the data was improved if the l parameter was optimized as well. The saturated water contents (θ_s) were fixed at 0.37 and 0.45 cm^3 cm^{-3} for the Lincoln and Columbia soils, respectively. The unsaturated hydraulic conductivity was not fixed at its measured value in the optimizations because the inverse solutions converged readily without K_s data. The variation in optimized K_s values (Table 2 and 3) is less than an order of magnitude, and as such could not be improved with a laboratory K_s measurement, which usually has an estimation error of similar magnitude. Also, we were interested in investigating dynamic phenomena, so including K_s data measured at steady-state conditions might confuse the issue.

Optimized parameters as well as squared residual (R^2) and sum of squared residual (SSQ) values for the different optimizations are listed in Table 2 and Table 3 for the Lincoln and Columbia soil, respectively. As seen in Table 2, the sum of squared residuals generally decreases with decreasing flow rate. For the Columbia soil in particular (Table 3), the SSQ values are significantly reduced when the exponent is allowed to vary (Case 2). For the Lincoln soil (Table 2) we observe an increase in the α values with decreasing flow rate, while the optimized n values are less sensitive to the flow rate. The increase in n values is not seen for the Columbia soil. These inversely obtained results reflect the trends observed for the

Table 3. Inversely estimated parameters for the Columbia soil. (1.) estimated parameters: (α, n, K_s, θ_r), (2.) estimated parameters: (α, n, K_s, θ_r, l).

Date	SSQ	θ_r	α	n	K_s (cm/h)	l	R^2
			Multistep 0–250–500 mbar				
0528a	0.045	0.040	0.010	1.634	1.050		0.995
0528b	0.001	0.186	0.007	3.655	0.140	-1.118	0.999
			Onestep 0–500 mbar				
0531a	0.039	0.036	0.010	1.604	1.005		0.993
0531b	0.012	0.187	0.007	3.582	0.143	-1.147	0.998
			Multistep 0–125–250–375–500 mbar				
0604a	0.029	0.041	0.011	1.561	1.128		0.999
0604b	0.008	0.186	0.010	2.830	0.187	-1.095	0.999

other estimation methods, which are discussed in the following.

RESULTS AND DISCUSSION
Soil Water Retention Characteristics

Fig. 3 shows the estimated average retention data obtained using both the direct (symbols) and inverse estimation (lines) approaches. We only present optimization data for the cases where l was optimized. Fig. 3a–d present the estimated retention data for each individual experiment, while Fig. 3e and 3f compare all directly estimated data (Fig. 3e) and optimized curves (Fig. 3f), respectively. It is evident from both Fig. 3e and 3f that soil water retention for the Lincoln soil is influenced by the drainage rate, regardless of the estimation method. In general, soil water retention increases as the number of pressure steps decreases, with the largest retention and residual water content for the single step experiment (0–250 mbar), and the lowest retention and residual water content for the quasi-static syringe pump and low-pressure multi-step outflow experiments. The differences were ≈7% by volume for a given matric potential in the early stages of the experiment. As we progress from the highest (0–250 mbar) to the lowest (quasi-static) flow rate, we also note a decrease in the measured air-entry value of ≈15 cm. Similar trends can be observed in the inversely estimated curves, suggesting that the directly estimated (measured) curves are representative of the average behavior of the sample. In contrast, no apparent rate dependence was observed for the fine textured Columbia soil (Fig. 4a–e). Generally, our measured curves for both the Lincoln and Columbia soil compare favorably with the curves measured by Chen et al. (1999).

Unsaturated Hydraulic Conductivity

The directly and inversely estimated unsaturated hydraulic conductivities are shown in Fig. 5 and 6 for the Lincoln and Columbia soil, respectively. Fig. 5a–d and Fig. 6a–c show a selection of the estimated unsaturated conductivity data for each individual experiment for the Lincoln and Columbia soils, respectively. Fig. 5e and 6d compare the directly estimated conductivity data as estimated using the bottom compartment drainage rates and matric potential gradients (K_3) for the Lincoln and Columbia soil, respectively. Fig. 5f and 6e present all

the inversely estimated curves for the two soils. Generally, the hydraulic conductivities computed using the two different estimation approaches (top down, K_{23} or bottom up, K_{32}) are very similar, thereby corroborating the K estimation methods. As mentioned previously, only data for the bottom (K_3) and middle (K_{23} and K_{32}) compartments are presented. In Figures 5a and 5b, we note a slight underestimation of the hydraulic conductivity, relative to the optimized conductivity curves, for the fast experiments, however, the data for the slower experiments (Fig. 5c and 5d) matched the optimized curves. A similar underestimation was determined for the Columbia soil (Fig. 6a–6c).

The estimated unsaturated hydraulic conductivity data for the different outflow experiments for the Lincoln soil are compared in Fig. 5e (direct, K_3) and 5f (inverse). The inversely estimated curves show an increase in hydraulic conductivity with increasing flow rate at high saturations. At high saturations at the start of the outflow experiments, differences in optimized hydraulic conductivity curves between the slow and fast outflow experiments are approximately one order of magnitude, with the highest conductivity values for the faster experiments (0–250 and 0–125, Fig. 5f). This trend is not so clearly apparent from comparison of the direct estimates (Figure 5e), because of lack of data points at high saturations for the fast outflow experiments; however, we would expect a similar behavior. As the sample water content decreases, this trend reverses with the highest unsaturated conductivity values (both optimized and directly computed) for the low flow-rate experiments. Similar trends were not observed for the Columbia soil (Fig. 6d and 6e) for which almost identical curves were obtained for the different drainage rates for both the inversely and directly computed estimates.

Physical Processes Controlling Outflow

A number of different physical processes might contribute to the rate-dependent results observed in our experiments. We suggest the following processes or a combination thereof, which systematically can explain the observed phenomena.

1. Entrapment of water. This is a plausible mechanism at high flow rates. We hypothesize that water entrapment occurs through hydraulic isolation of water-filled pores by draining surrounding pores. The larger the drainage rate, the less opportunity

Lincoln
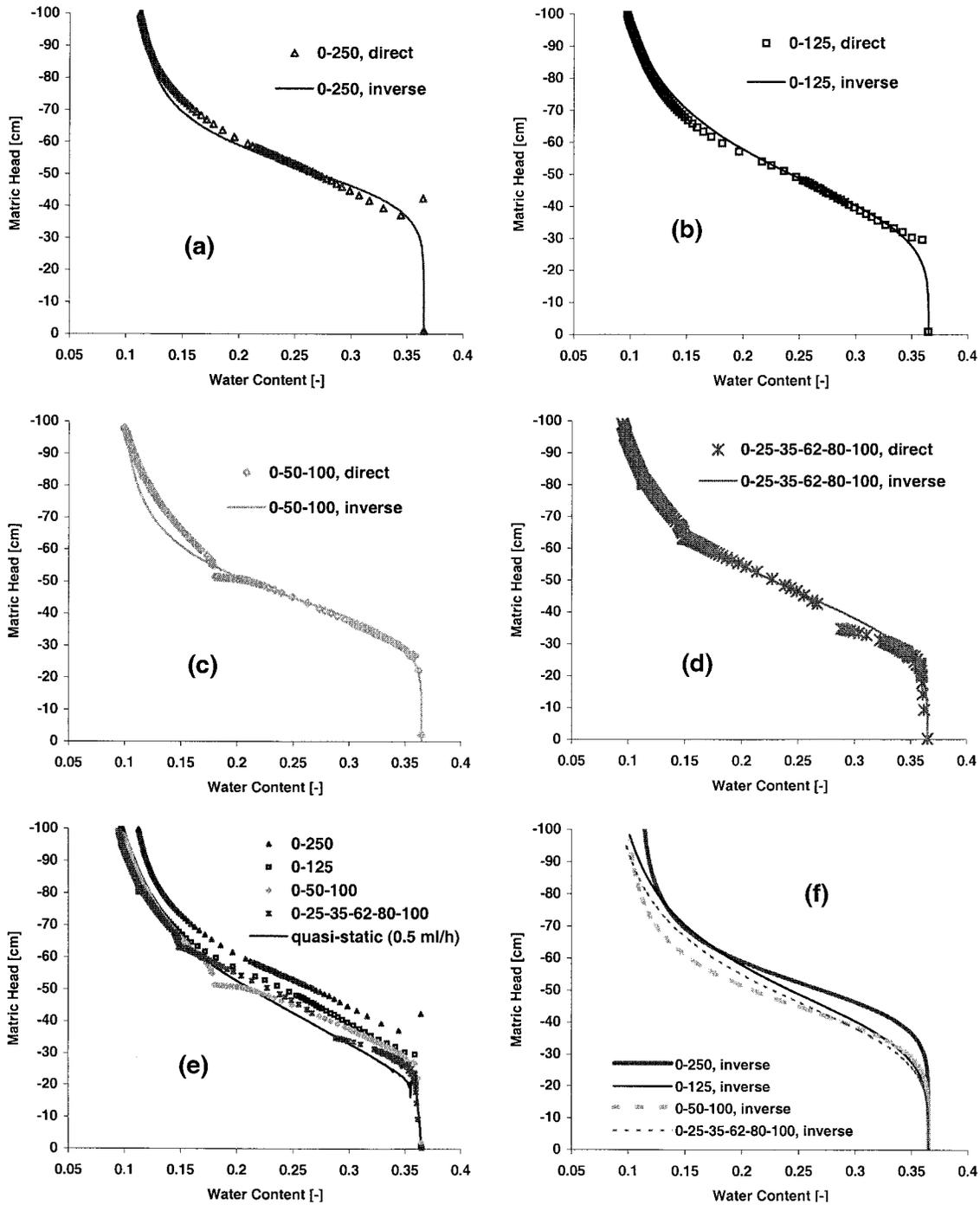
Fig. 3. Directly and inversely estimated retention curves for the Lincoln soil as a function of applied pressure (a) 0–250 mbar, (b) 0–125 mbar, (c) 0–50–100 mbar, (d) 0–25–35–62–80–100 mbar, (e) directly estimated curves for all experiments, (f) inversely estimated curves for all the experiments.

exists for all pores to drain concurrently. It may occur throughout the soil sample and will increase water retention, but will decrease unsaturated hydraulic conductivity, as the mobile portion of the soil water is decreased. The highest flow rates occur for one-step experiments and for coarse-textured soils, and hence water entrapment is likely

to be more prevalent in coarse soils with large head gradients.

2. Pore water blockage. When applying a sudden large pressure step to a near-saturated or saturated soil sample, the large matric potential head gradients near the porous membrane result in faster drainage of the pores at the bottom of the sample

Columbia
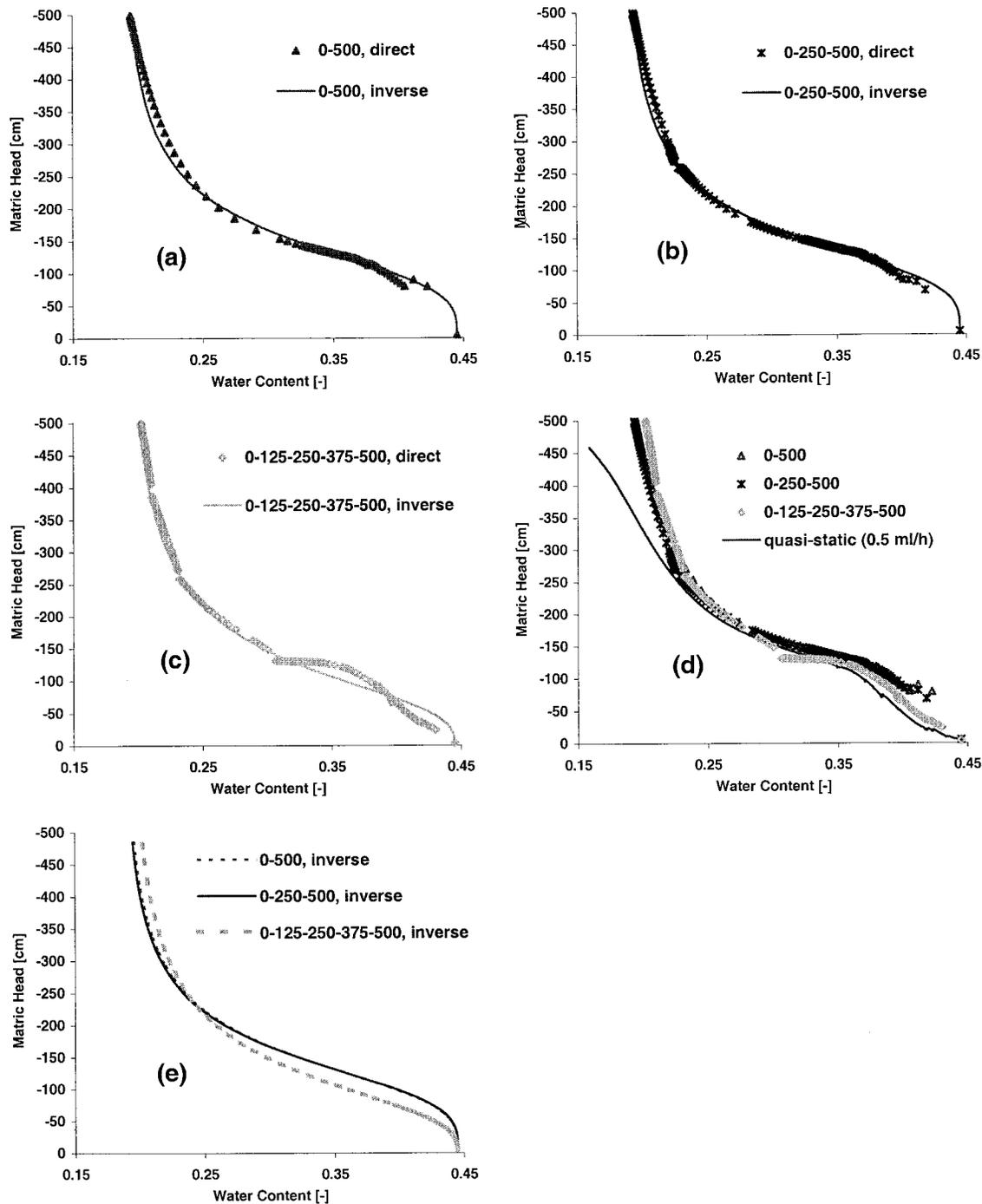
Fig. 4. Directly and inversely estimated retention curves for the Columbia soil as a function of applied pressure (a) 0–500 mbar, (b) 0–250–500 mbar, (c) 0–125–250–375–500 mbar, (d) directly estimated curves for all experiments, (e) inversely estimated curves for all the experiments.

than in the overlying soil, thereby isolating the conductive flow paths and impeding further drainage and equilibration of the soil. Consequently, the sample's unsaturated hydraulic conductivity will be reduced. Pore blockage is likely to occur for materials with a uniform pore size distribution (like the Lincoln sand). It is assumed that air is available

to replace the draining water at the bottom of the sample, hence it can only occur if there is macroscopic air continuity across the whole sample (air entry value of soil must be exceeded).

3. Air entrapment. This mechanism was discussed by Schultze et al. (1999) who used a two-fluid numerical code to model their results, thereby accounting

Lincoln
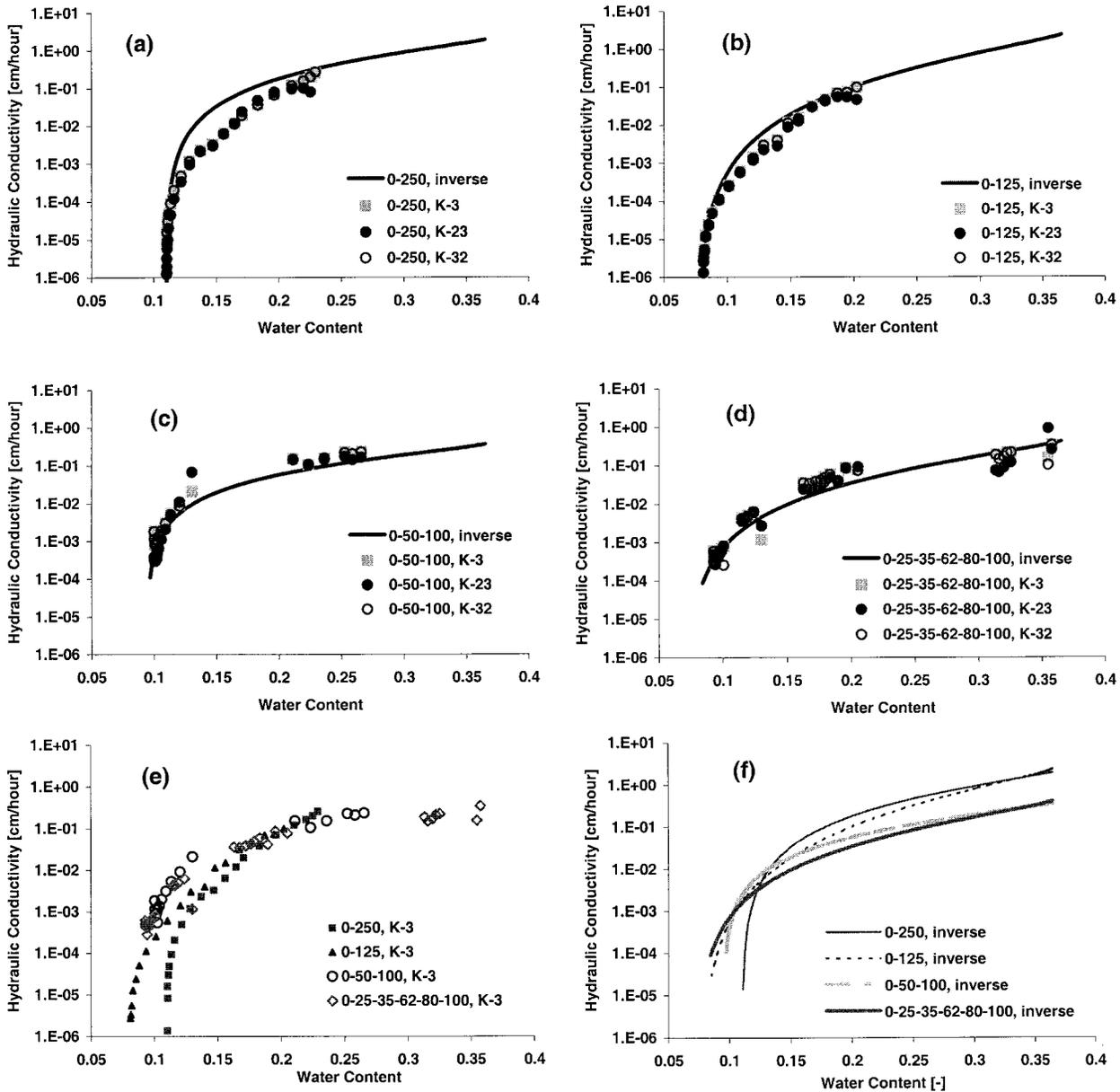
Fig. 5. Directly and inversely estimated unsaturated hydraulic conductivity curves for the Lincoln soil as a function of applied pressure (a) 0–250 mbar, (b) 0–125 mbar, (c) 0–50–100 mbar, (d) 0–25–35–62–80–100 mbar (only the curves for the middle and bottom compartments are shown), (e) directly estimated curves for all experiments for the bottom part of the sample (K_3), (f) inversely estimated curves for all experiments.

for spatial and temporal changes in air pressure in the sample. When a soil core is drained either by increasing the gas phase pressure or by decreasing the water phase pressure, it is generally assumed that air is available to replace the draining water; however, for a sample holder that is open to air only at the top of the soil sample, this assumption of air phase continuity throughout the sample is not necessarily valid. According to Corey and Brooks (1999), initial drainage for such or similar conditions will occur as a result of depression of interfaces at the sample holder boundaries or by

a slight expansion of entrapped gas, instead of air replacing draining water. As pointed out by Schultze et al. (1999), air entrapment can increase water retention. Air entrapment is more likely if air permeability is low at high water saturation. As a result, soil water retention will be nonunique, and is determined by the rate of pressure step changes. Also, as was demonstrated by Schultze et al. (1999), the trapped air will effectively decrease cumulative drainage and drainage rate, and result in reduced unsaturated hydraulic conductivity values at near saturation. Regarding the use of either

Columbia
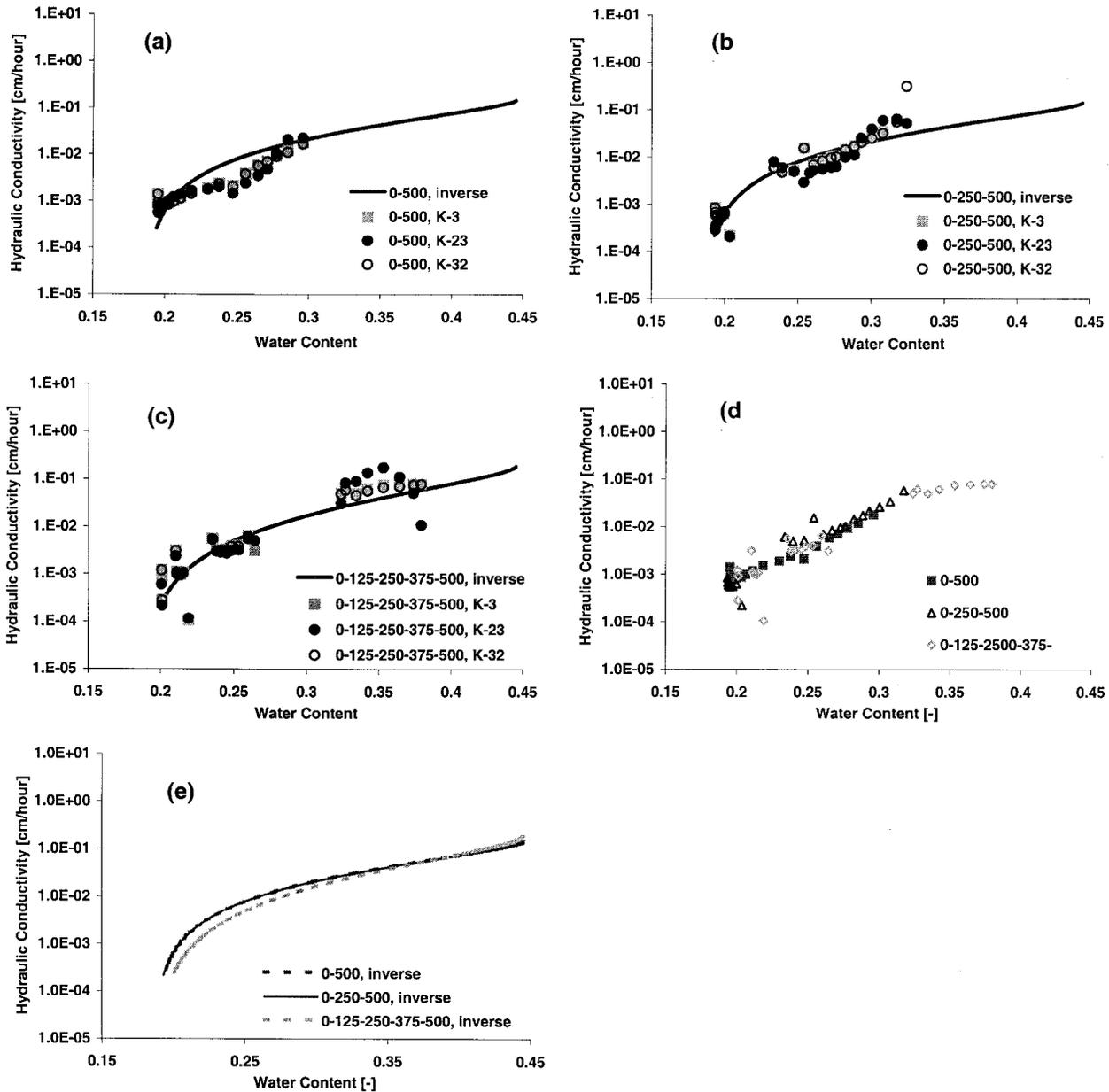
Fig. 6. Directly and inversely estimated unsaturated hydraulic conductivity curves for the Columbia soil as a function of applied pressure (a) 0–500 mbar, (b) 0–250–500 mbar, (c) 0–125–250–375–500 mbar, (d) directly estimated curves for all experiments for the bottom part of the sample (K_3), (e) inversely estimated curves for all experiments. (Only the curves for the middle and bottom compartments are shown).

air phase pressure or water phase suction to induce outflow, Eching and Hopmans (1993) measured retention curves using both suction and air pressure experiments and found relatively small differences between the two approaches; however, we acknowledge that there are additional complexities regarding the suction vs. pressure issue for instance as discussed by Chahal and Young (1965) and Peck (1960).

4. Air-entry value effect. This phenomenon is present when dynamic flow experiments are carried out

while the soil in the pressure cell (with porous membrane) is saturated as occurs when the air entry value of the soil is not exceeded prior to applying the first pressure step. The lack of continuity in the gas phase will cause piston-type flow, with drainage occurring from the top, rather than the bottom (Hopmans et al., 1992). This process is mostly effective if the soil has a distinct air entry value. It will increase unsaturated K near saturation, however, it is not clear how it will affect water retention. Also, according to Corey and Brooks

(1999), matric potentials cannot be measured for saturations above ≈85%, because of the general disconnection of the gas phase at these high saturations. Consequently, one would expect nonunique soil water retention curves, controlled by imposed boundary conditions and pore connectivity characteristics.

5. Dynamic contact angle effect. Friedman (1999) hypothesized that the advancing or receding solid–liquid–gas contact angle in a capillary tube is dependent on the velocity of the propagating or withdrawing liquid–gas interface. Hence, in dynamic experiments, the static contact angle has to be replaced with a dynamic contact angle. Although in concept possible, Friedman agrees that such explanation is probably for fluids with low interfacial tensions such as NAPL water. For draining soil samples, a reduction of the contact angle in the range between 0 and 30° has a limited influence on the matric potential, as increasing flow velocities would decrease that contact angle to a minimum value of zero. Hence, the contact angle effect will be small in any case for draining soils. Moreover, although the contact angle effect can explain the increasing water retention with increasing flow velocities, it can not explain the increasing unsaturated hydraulic conductivity with increasing water velocities.

Observed Phenomena in the Context of the Suggested Processes

We suggest that the marked effect on the curves for the Lincoln soil can be attributed to three or four of the above stated mechanisms. The first mechanism is caused by disconnection of flow paths at higher flow rates, so that water is being trapped in dead-end pore space, Process 1. For the low-pressure outflow experiments, water in individual pores remains connected to the bulk water, thereby allowing water to drain as the water potential decreases during multi-step outflow experiments. A similar explanation has been suggested earlier by Smiles et al. (1971) and Topp et al. (1967).

In addition to water entrapment, we believe that Processes 2, 3 and 4 contribute to the measured rate-dependent soil hydraulic characteristics. Initial drainage of the lower part of the sample (Process 2) was observed in one-step outflow experiments using x-ray computer assisted tomography (CT) by Hopmans et al. (1992) and we are currently observing similar patterns in preliminary x-ray CT experiments of the Lincoln soil. This mechanism is enhanced for soils with a narrow pore-size distribution, and hence is expected to be more pronounced for the sandy Lincoln soil. Similarly, the air-entry value effect (Process 4) is likely to influence our results, since the air entry value of the Lincoln soil is ≈−20 cm; that is, drainage occurs only if matric potential head values are smaller than −20 cm; however, the initial condition of the soil was only ≈−2 cm, so that the first pressure increment was applied when the Lincoln soil was still saturated. This is particularly critical

for the Lincoln soil experiments with large pressure increments (one or two steps) where early drainage most likely did not conform to Richards type of flow, which assumes that the nonwetting or air phase is continuous throughout the soil sample (Hopmans et al., 1992). Also, Schultze et al. (1999) stated that the air phase is discontinuous during drainage until a significant amount of water has left the pore system and an emergence point saturation is reached, at which point the gas permeability jumps to a finite value.

The influence of flow rate on the retention characteristic was not apparent for the finer textured Columbia soil (Fig. 4a–e) using different applied pressures; however, we hypothesize that a similar behavior might have occurred if much higher gas pressures had been applied to drain the Columbia soil than used in the reported experiments. Chen et al. (1999) showed that the air permeability is higher for the Columbia soil than for the Lincoln soil, at the same degree of saturation. Therefore, some of the above processes, which are controlled by the low air permeability and the lack of air phase continuity of the Lincoln soil, might not be of importance for the Columbia soil. Another reason for the relatively small deviations among the retention curves for the Columbia soil, could be the small matric potential gradients present later in the experiment (i.e., at lower saturations). Fig. 7 and 8 illustrate matric potential gradients as estimated directly from the two tensiometers for the Lincoln and Columbia soils, respectively. As seen from Fig. 8, the directly estimated matric potential gradients in the Columbia soil (solid lines) are large at first following an applied pressure increment, but quickly drop to ≈−1.0, as is expected if hydraulic equilibrium is attained. The periodic return of the matric potential gradients to near zero for the Columbia soil is the result of the total soil water potential approaching static conditions after each of the applied pressure increments; however, the return to static equilibrium after each applied pressure increment does not always occur for the sandy soil, especially not for the high-pressure single step experiments as illustrated in Fig. 7. The continuously increasing matric potential gradient (solid lines) is indicative of a soil water regime not tending towards static equilibrium. Our proposed mechanism, Process 2, can explain this phenomenon. After a large pressure increment is applied, the bottom section of the sandy soil is drained, thereby emptying the largest, highly conductive pores. For a soil with a narrow pore size distribution (Lincoln soil), drainage of the largest pores prevents continued drainage and equilibration of the soil above the initially drained portion, and effectively results in the increasing total water potential gradients with progressing drainage as observed in Fig. 7. For the two slower outflow experiments (0–50–100 mbar and 0–25–35–62–80–100 mbar), a similar behavior as for the finer textured soil is observed, and the gradients return to unity, shortly after the pressure step is applied.

In general, the numerical model simulated total matric potential heads similar to what was observed, even for the fast outflow experiments (compare solid with dashed lines in Fig. 7 and 8). Extended forward model-
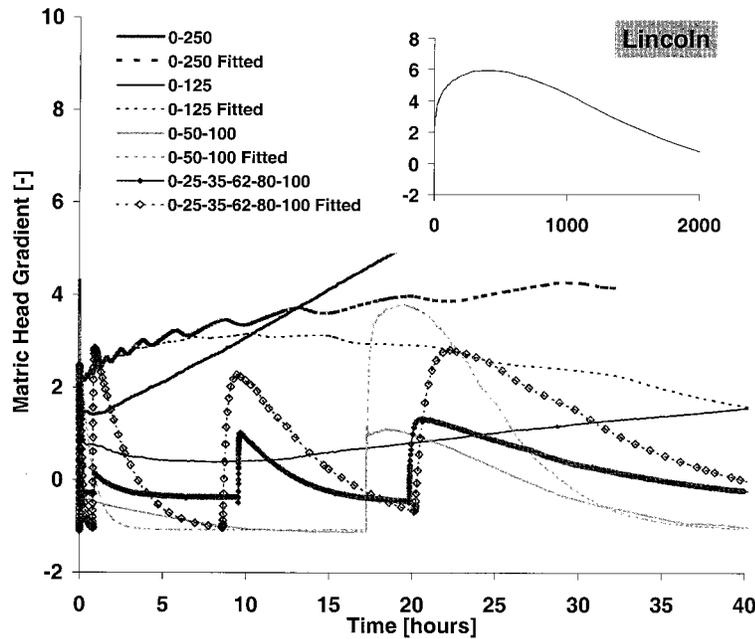
Fig. 7. Matric potential gradients measured and optimized between the two tensiometers in the Lincoln soil.

ing of the 0–250 mbar experiment for the Lincoln soil showed that static equilibrium is not approached until 2000 hours or ≈83 days have passed (see inset of Fig. 7). Generally, when performing retention curve measurements on sandy materials it is assumed that these can be done relatively fast, whereas the more clayey materials require time-consuming experiments; however, our results indicated otherwise.

At low saturations, we observed low unsaturated hydraulic conductivities for the fast outflow experiments for the Lincoln soil, Fig. 5e and Fig. 5f. We suggest that this is due to water being either trapped (Process 1) or blocked from the main water body (Process 2), thereby becoming immobile and effectively not contributing to flow. We hypothesize that this water becomes entrapped and immobile in the early stages of the experiment when relatively high flow rates prevail, particularly in those experiments where large one-step pressure steps were used to induce outflow. In Fig. 9, the cumulative outflow volumes are plotted as a function of time for the Lincoln soil, showing that the maximum flow rates occur initially when the first pressure increment is applied. We assume that these maximum flow rates occur near the nylon membrane at the bottom of the sample. Specifically, the 0–250 and 0–125 drainage experiments induce these high flow rates in the first few minutes of the experiment (see inset of Fig. 9). The initially trapped or blocked water will remain trapped as the soil continues to drain because it is disconnected from the flowing water phase. Another possible reason for the negligible effect of the outflow rate on the hydraulic characteristics of the Columbia soil is its dominance of smaller pores following our proposed Process 1. Single water-filled pores are less likely to be isolated from the main flow path in the Columbia soil, compared with the coarser textured Lincoln soil.

At high saturations, we observed higher conductivi-

ties for the faster experiments (Fig. 5e and 5f). Similar results were found by Plagge et al. (1999) and Schultze et al. (1999), and we believe that the main cause of these increased conductivities derives from our proposed Process 4. If the air pressure is suddenly increased (or the water pressure decreased as in the case of the experiments of Plagge et al. (1999) and Schultze et al. (1999) without first exceeding the air entry value of the soil, thereby providing air passage into the soil, water will drain from the sample relatively fast and the unsaturated hydraulic conductivity will be overestimated. However, at the later stages of drainage, the water entrapment effect and pore blockage becomes the controlling factor in the hydraulic conductivity estimation, and a crossover of the curves in Fig. 5e and 5f is observed. Apparently, this crossover occurs at a lower saturation in the in-
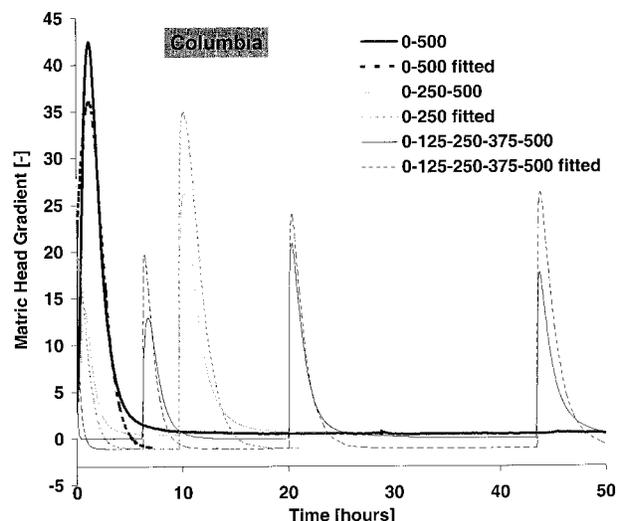
Fig. 8. Matric potential gradients measured and optimized between the two tensiometers in the Columbia soil.
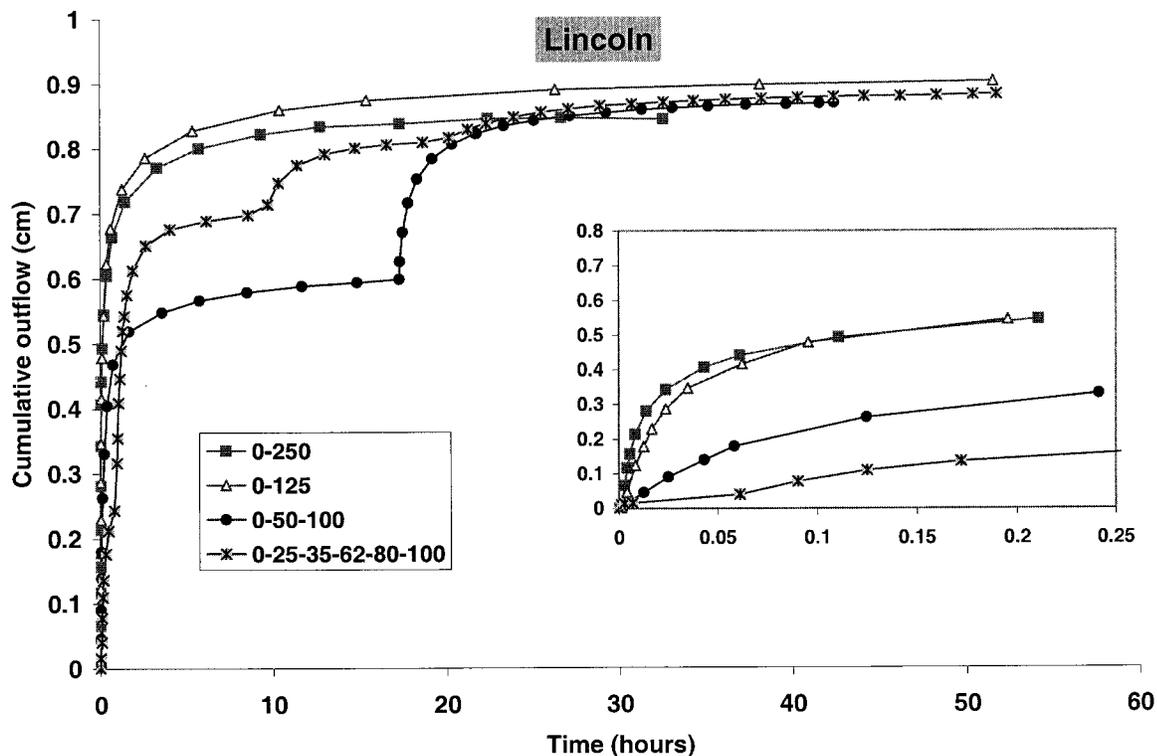
Fig. 9. Cumulative outflow rates as a function of time for the Lincoln soil. Early time data is shown in inset.

versely estimated curves (between water contents of $0.10–0.15 \, cm^3 \, cm^{-3}$), while the directly estimated curves show a crossover point at a water content of $\approx 0.20 \, cm^3 \, cm^{-3.}$ The inversely estimated data is based on the assumption of Richards flow and air phase continuity, which could be the cause of this difference between the direct and indirect unsaturated hydraulic conductivity calculations.

The crossover of the hydraulic conductivity curves is not observed for the finer textured Columbia soil in Figure 6e, likely due to its more poorly defined air-entry value (Process 4), wider pore-size distribution (Process 1 and 2), and higher air permeability (Process 3). Also, the measurements of the finer-textured Columbia soil do not show the continuously increasing nonequilibrium gradients as measured for the Lincoln soil (compare Fig. 7 and 8), and therefore the hydraulic characteristics of this soil are less likely to be dependent on flow rate. The lower initial flow rates and their smaller variation among the Columbia experiments are illustrated in Fig. 10 (note that the inset is plotted on the same scale for the two soils).

CONCLUSIONS

In conclusion, we believe that the rate-dependent phenomena observed for the coarse Lincoln soil in these experiments are a consequence of a combination of flow processes, and are a result of differences in pore size distribution and pore connectivity between the two soils. Process 4 mainly affects the unsaturated hydraulic conductivity curve at high water contents, while the accompanying high flow rates trap (Process 1) and block (Proc-

ess 2) water, thereby affecting soil water retention. All of these phenomena are mostly prevalent in the coarse textured soil and for the high flow rates. As the soil desaturates, Process 4 is no longer a factor, however, it is the entrapped and blocked water that controls the hydraulic properties, thereby reducing the unsaturated hydraulic conductivity in the lower water content range. Our explanations can be applied to results presented by others. For example, both Plagge et al. (1999) and Schultze et al. (1999) found increased hydraulic conductivities with increasing flow rates that can be explained from Process 4. Also, the results of Topp et al. (1967) can be explained using the air entrapment argument (Process 4), as their drainage experiments were initiated at full saturation while the soil's air entry value was $\approx -35 \, cm$. In the experiments of Smiles et al. (1971), air access was secured at any time because the sample holder included ventilation holes. However, their experiments confirm Process 1 to be effective. Water retention is highest closest to the water inlet (largest fluxes) and for experiments with the largest head gradients (Fig. 4 and 6). The results of Smiles et al. (1971) were confirmed by Vachaud et al. (1972), who showed that the largest deviations from the static water retention curve occur when large head gradients are applied (Process 1 and 2).

Based on our investigation it is critical to consider the method by which the hydraulic properties for unsaturated soils are determined, thus keeping in mind the purpose of the characterization. For the coarse textured Lincoln soil we have shown that the use of hydraulic parameters obtained under relatively high outflow conditions may not accurately represent slow flow phenom-
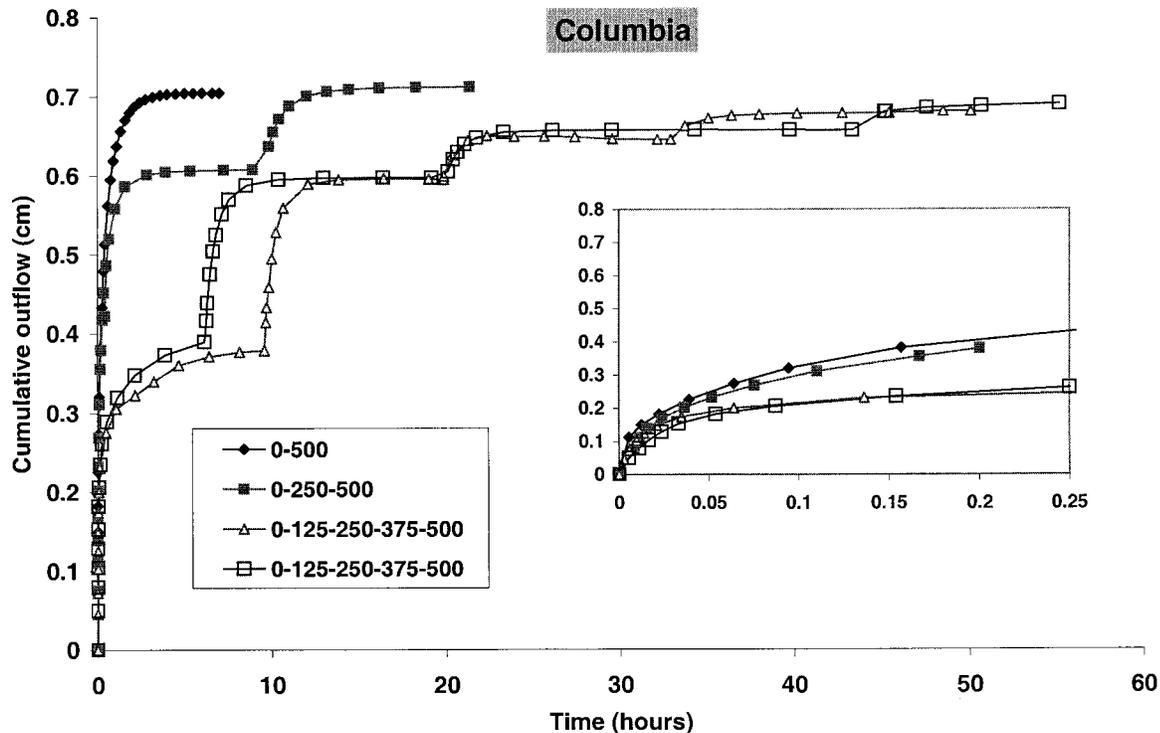
Fig. 10. Cumulative outflow rates as a function of time for the Columbia soil. Early time data is shown in insert.

ena, as mostly experienced in the field. The lack of static equilibrium in the coarser soil material may affect both inverse and direct estimations. Therefore, the choice of boundary conditions and estimation method must be carefully evaluated.

The rate dependence of the hydraulic characteristics has been shown to be of less importance for the finer textured Columbia soil, at least for the experimental conditions investigated in this study. The higher air permeability for the Columbia soil at a given saturation, along with its wider pore-size distribution and a more poorly defined air entry value are likely reasons for the lack of rate dependence observed for the Columbia soil. Also, the induced flow rates in the Columbia soil experiments were not as high as those measured for the Lincoln soil. Therefore, it is possible that some of the flow rate effects on the soil hydraulic characteristics are effective for the Columbia soil as well, if higher flow rates were used by applying much larger water pressure gradients than used in this study.

We realize that other processes such as those stated for instance by Demond and Roberts (1991), Hassanizadeh and Gray (1993), Clayton (1999), and Friedman (1999) may also be contributing to the observed flow rate dependent soil hydraulic properties. Regardless, ignoring these rate-dependent phenomena might lead to significant errors, especially in situations where hydrological models are used with hydraulic parameters that are obtained at considerably different flow rates.

REFERENCES

Clayton, W.S. 1999. Effects on pore scale dead-end air fingers on relative permeabilities for air sparging in soils. Water Resour. Res. 35:2909–2919.

Chahal, R.S., and R.N. Young. 1965. Validity of soil characteristics determined with the pressure apparatus. Soil Sci. 99:98–103.

Chen, J., J.W. Hopmans, and M.E. Grismer. 1999. Parameter estimation of two-fluid capillary pressure-saturation and permeability functions. Adv. in Water Resour. 22:479–493.

Corey, A.T., and R.H. Brooks. 1999. The Brooks-Corey relationships. p. 13–18. In M. Th. van Genuchten, F.J. Leij, and L. Wu (ed.) Proc. of the International Workshop on Characterization and Measurement of the Hydraulic Properties of Unsaturated Porous Media. 22–24 Oct. 1997. Univ. of California. Riverside, CA.

Davidson, J.M., D.R. Nielsen, and J.W. Biggar. 1966. The dependence of soil water uptake and release upon the applied pressure increment. Soil Sci. Soc. Am. Proc. 30:298–304.

Demond, A.H., and P.V. Roberts. 1991. Effect of interfacial forces on two-phase capillary pressure-saturation relationships. Water Resour. Res. 27:423–437.

Eching, S.O., and J.W. Hopmans. 1993. Optimization of hydraulic functions from transient outflow and soil water pressure data. Soil Sci. Soc. Am. J. 57:1167–1175.

Eching, S.O., J.W. Hopmans, and O. Wendroth. 1994. Unsaturated hydraulic conductivity from transient multistep outflow and soil water pressure data. Soil Sci. Soc. Am. J. 58:687–695.

Friedman, S.P. 1999. Dynamic contact angle explanation of flow rate-dependent saturation-pressure relationships during transient liquid flow in unsaturated porous media. J. Adhesion Sci. Technol. 13:1495–1518.

Harris, C.C., and N.R. Morrow. 1964. Pendular moisture in packings of equal spheres. Nature 203:706–708.

Hassanizadeh, S.M., and W.G. Gray. 1993. Thermodynamic basis of capillary pressure in porous media. Water Resour. Res. 29:3389–3405.

Hollenbeck, K.J., and K.H. Jensen. 1999. Dependence of apparent unsaturated parameters on experiment type and estimation method. p. 913–922. *In* M. Th. van Genuchten, F.J. Leij, and L. Wu (ed.) Proc. of the Int. Workshop on Characterization and Measurement of the Hydraulic Properties of Unsaturated Porous Media, 22–24 Oct. 1997. Univ. of California. Riverside, CA.

Hopmans, J.W., T. Vogel, and P.D. Koblik. 1992. X-ray tomography of soil water distribution in one-step outflow experiments. Soil Sci. Soc. Am. J. 56(2):355–362.

Hopmans, J.W., and J. Simunek. 1999. Review of inverse estimation of soil hydraulic properties. p. 643–659. *In* M. Th. van Genuchten, F.J. Leij, and L. Wu (ed.) Proc. of the Int. Workshop on Characterization and Measurement of the Hydraulic Properties of Unsaturated Porous Media, 22–24 Oct. 1997. Univ. of California. Riverside, CA.

Klute, A. (ed.) 1986. Methods of soil analysis. Part 1. 2nd. ed. Agron. Monogr. 9. ASA and SSSA, Madison, WI.

Kool, J.B., J.C. Parker, and M.Th. van Genuchten. 1985. Determining soil hydraulic properties from one-step outflow experiments by parameter estimation: 1. Theory and numerical studies, Soil Sci. Soc. Am. J. 49:1348–1354.

Liu, Y.P., J.W. Hopmans, M.E. Grismer, and J.Y. Chen. 1998. Direct estmation of air-oil and oil-water capillary pressure and permeability relations from multi-step outflow experiments. J. Contam. Hydrol. 32:223–245.

Mualem, Y. 1976. A new model for predicting the hydraulic conductivity of unsaturated porous media, Water Resour. Res. 12:513–522.

Nielsen, D.R., J.W. Biggar, and J.M. Davidson. 1962. Experimental consideration of diffusion analysis in unsaturated flow problems. Soil Sci. Soc. Am. Proc. 26:107–111.

Peck, A.J. 1960. Change of moisture tension with temperature and air pressure. Theoretical Soil Sci. 89:303–310.

Plagge, R., P. Häupl, and M. Renger. 1999. Transient effects on the hydraulic properties of porous media. *In* M. Th. Van Genuchten, F.J. Leij, and L. Wu (ed.) Proc. of the Int. Workshop on Characterization and Measurement of the Hydraulic Properties of Unsaturated Porous Media. Oct. 22–24, 1997. Univ. of California. Riverside, CA.

Schultze, B., O. Ippisch, B. Huwe, and W. Durner. 1999. Dynamic nonequilibrium during unsaturated water flow. p. 877–892. *In* M. Th. Van Genuchten, F.J. Leij, and L. Wu (ed.) Proc. of the Int. Workshop on Characterization and Measurement of the Hydraulic Properties of Unsaturated Porous Media. Oct. 22–24, 1997. Univ. of California. Riverside, CA.

Simunek, J., M. Sejna, and M.Th. van Genuchten. 1998. The HYDRUS-1D software package for simulating the one-dimensional movement of water, heat and multiple solutes in variably-saturated Version 2.0, IGWMC-TPS-70, Int. Ground Water Modeling Center, Colorado School of Mines, Golden, CO, 202p.

Smiles, D., G. Vachaud, and M. Vauclin. 1971. A test of the uniqueness of the soil moisture characteristic during transient non hysteretic flow of water in a rigid soil. Soil Sci. Soc. Am. Proc. 35:534–539.

Topp, G.C., A. Klute, and D.B. Peters. 1967. Comparison of water content-pressure head data obtained by equilibrium, steady-state and unsteady state methods. Soil Sci. Soc. Am. Proc. 31:312–314.

Vachaud, G., M. Vauclin, and M. Wakil. 1972. A study of the uniqueness of the soil moisture characteristic during desorption by vertical drainage. Soil Sci. Soc. Am. Proc. 36:531–532.

van Dam, J.C., J.N.M. Stricker, and P. Droogers. 1994. Inverse method to determine soil hydraulic functions from multistep outflow experiments. Soil Sci. Soc. Am. J. 58:647–652.

van Genuchten, M.Th. 1980. A closed-form equation for predicting the hydraulic conductivity of unsaturated soils. Soil Sci. Soc. Am. J. 44:892–898.

Wendroth, O., W. Ehlers, J.W. Hopmans, H. Kage, J. Halbertsma, and J.H.M. Wösten. 1993. Reevalution of the evaporation method for determining hydraulic functions in unsaturated soils. Soil Sci. Soc. Am. J. 57:1436–1443.

Wildenschild, D., K.H. Jensen, K.J. Hollenbeck, T.H. Illangasekare, D. Znidarcic, T. Sonnenborg, and M.B. Butts. 1997. A two-stage procedure for determining unsaturated hydraulic characteristics using a syringe pump and outflow observations. Soil Sci. Soc. Am. J. 61:347–359.